

# Capillary Pressure Behavior of CO<sub>2</sub> - Shale System at Elevated Temperatures

Original Research Article

## ABSTRACT

In this study, changes in capillary entry pressure of shale when interacting with CO<sub>2</sub>, under different temperatures have been investigated. The combined impact of temperature and petrophysical properties of shale (water content, water activity, permeability and porosity) on capillary entry pressure was addressed. Pressure breakthrough measurements were used to evaluate the minimum entry pressure of CO<sub>2</sub> through shale. A heavy-duty oven was used to vary the temperature in order to investigate the impact of temperature on CO<sub>2</sub> capillary entry pressure through shale. Results showed that capillary entry pressure of shale when interacting with CO<sub>2</sub> was highly affected by temperature. Higher temperatures decreased capillary entry pressure of shale. We believe that pore dilation, where pore throat size expands due to the application of heat, may have caused this decrease in capillary entry pressure. However, in some cases higher temperature activated clay swelling that may have caused an apparent decrease in pore throat radii of shale which translated into higher capillary entry pressure. Results also showed that there exists no distinct relationship between petrophysical properties of shale and its measured capillary entry pressure when interacting with CO<sub>2</sub> at different temperatures. Heat could alter pore throat radii and cause pore dilation which may alter measured capillary entry pressure. Interfacial tension decreases with increasing temperature and that can be attributed to the weakening of intermolecular forces at the two immiscible fluids interface. Swelling of clay could be related to temperature-induced transition from passive to an active clay.

*Keywords: Depleted reservoirs; CO<sub>2</sub> sequestration; pore dilation; clay swelling; shale sealing capacity; entrance pressure.*

## ABBREVIATION

$P_c$  : Capillary entry pressure.  
 $P_{CO_2}$  : Pressure in CO<sub>2</sub> phase.  
 $P_{water}$  : Pressure in water phase.  
 $\sigma$  : Interfacial tension between CO<sub>2</sub> and water.  
 $\theta$  : Contact angle.  
 $r$  : Shale's pore throat radius.  
 $h$  : Sealing capacity of shale.  
 $P_{c,min}$  : Minimum capillary entry pressure.  
 $\rho_w$  : Density of water.  
 $\rho_o$  : Density of oil.  
 $g$  : Acceleration due to gravity.  
 $\phi$  : Shale's porosity.  
 $k$  : Shale's permeability.

## 1. INTRODUCTION

The idea of reducing the concentration of carbon dioxide (CO<sub>2</sub> sequestration) in the atmosphere is receiving increasing attention by scientists and policy makers around the world. CO<sub>2</sub> is a

hazardous "greenhouse" gas where it absorbs and emits infrared radiation, warms the earth's surface and lowers the levels of oxygen in the atmosphere. CO<sub>2</sub> sequestration is simply defined as catching and storing carbon in geologic formations, or underground aquifers to reduce its concentration in atmosphere. This operation will need a solid scientific foundation defining the coupled hydrologic-geochemical-geomechanical processes that govern the long-term fate of CO<sub>2</sub> in the subsurface [1]. The captured CO<sub>2</sub> would then be separated, transported and stored either in the ocean or injected underground in deep depleted reservoir formations with high porosity [2]. The second option, deep depleted reservoir formations, is the purpose of our project. This option requires methods to characterize and select sequestration sites, subsurface engineering to optimize performance and cost, approaches to ensure safe operation, monitoring technology, remediation methods, regulatory overview, and an institutional approach for

managing long-term liability [3]. In order to understand the mechanism of storing carbon dioxide in deep reservoir formations, several concepts are required to be clarified.

### 1.1 Subsurface Traps

Subsurface traps are below ground traps where a permeable reservoir rock (high porosity) is overlaid by low permeability caprocks. Caprocks can take several forms, but they all prevent the upward migration of fluids to surface. When any fluid reaches the reservoir rock, they continue to migrate upwards through the pore spaces of the rock until blocked by seal barrier (caprock). The low permeability caprocks are generally shale or low permeability sandstones and carbonate rocks [4].

### 1.2 Shale Caprocks

The primary sequestration mechanism during at least the first decades, is the caprocks, which can be explained from the understanding of the structure of traps, where a caprock acts as a sealing barrier to prevent the CO<sub>2</sub> migration and leakage to surface. The efficiency of CO<sub>2</sub> sequestration depends on the sealing properties of the caprock. For example, shale plays an important role in petroleum exploration and production because it can be found in nature as source rocks or caprocks. This characteristic promoted shale as a good candidate for CO<sub>2</sub> sequestration operation. Shales are important for the process of CO<sub>2</sub> sequestration because they are underground seals that can stop the flux of CO<sub>2</sub> through it. As a result of their low permeability, high capillary forces are created to prevent CO<sub>2</sub> from breaking through shale caprock as shown in Fig. 1. The capillary entry pressure of shale is the pressure at which non-wetting fluids such as CO<sub>2</sub> can enter shale caprocks. Shale capillary entry pressure plays an important role when searching for potential depleted reservoirs to store captured CO<sub>2</sub> [5]. Measurements of capillary entry pressure will help in quantifying the sealing capacity of shale caprock.

### 1.3 Capillary Entry Pressure

In definition, the capillary entry pressure is the maximum pressure difference that may exist across the interface that separates two immiscible fluids before the non-wetting fluid penetrates the pore space [7]. It can be calculated as the pressure of the non-wetting phase (such as CO<sub>2</sub>) minus the pressure of the wetting phase (pore fluid). The wettability

depends on its surface tension which can be defined as, the ability of one fluid to stick to a solid surface in the existence of other immiscible fluids, and it can be determined through the contact angle of the fluid [8]. The capillary pressure that exists between two immiscible fluids is given by:

$$P_c = P_{CO_2} - P_{water} = \frac{2\sigma\cos\theta}{r} \quad (1)$$

As it is clear from equation 1, for CO<sub>2</sub> to enter a shale, the differential pressure between the CO<sub>2</sub> and water must exceed the minimum capillary entry "threshold" pressure of the shale. The minimum capillary entry pressure in definition is the capillary pressure at which the non-wetting phase, usually oil or gas, starts to displace the wetting phase, usually brine, contained in the largest pore throat within a water-wet formation [9]. According to equation 1, the capillary entry pressure can be significant, for very small pore throats shales (permeability). The minimum capillary entry pressure can also be used to estimate the height of a hydrocarbon column that can be trapped by a shale caprock. At equilibrium, the height of the hydrocarbon column, also called the sealing capacity, is given by the following equation:

$$h = \frac{P_{c,min}}{(\rho_{water} - \rho_{oil})g} \quad (2)$$

It can be seen from equation 2 that the minimum capillary entry pressure ( $P_{c,min}$ ) must be known in order to estimate the sealing capacity of shale (h).

### 1.3 Factors Affecting Capillary Entry Pressure

There are direct and indirect factors that affect the capillary entry pressure. The direct factors can be obtained from equation (1) where capillary entry pressure depends on both the water-wet shale and the non-wetting fluid properties. More specifically, the capillary entry pressure depends on the interfacial tension between the shale pore fluid and the non-wetting fluid, the contact angle, and the shale pore throat radius. The indirect factors that affect the capillary entry pressure are the reservoir physical and geometric properties (e.g., entry value, permeability, layering, heterogeneity and spatial correlation, anisotropy, and dipping), injection rate and pressure [10]. Also, in situ pressure and temperature affects the capillary entry pressure of shale since the density of CO<sub>2</sub> is highly affected by both pressure and temperature [11].

### 1.4 Methods of Evaluating Capillary Entry Pressure

Capillary entry pressure of caprocks is measured by two different methods. The first method is direct laboratory scale injection that can be done on core samples, and the second method is indirect methodologies that are typically based on the evaluation of the material pore size, wettability, and mineralogical composition; however, they are limited by the testing conditions, calling into question the consistency of the determined capillary entry-pressure [12].

Many articles related to “CO<sub>2</sub> sequestration”, especially in depleted reservoirs, and the methodologies used to measure the capillary entry pressure of caprocks particularly shales were studied and investigated. It has been noticed that it is important to understand how the CO<sub>2</sub> behaves during the sequestration under two conditions, high pressure and high temperature, to accomplish an effective and safe storage of the overlaying caprock. However, in most of the previous studies the first condition, high pressure, had been taken into consideration while the second condition, high temperature, had been largely ignored. In this report, the effect of thermal changes on capillary entry pressure will be examined.

## 2. LITERATURE REVIEW

Different studies discussed different parameters that can affect the capillary pressure of different fluids in shale [13] were studying the impact of CO<sub>2</sub> injection on the hydro-mechanical behavior of a clay-rich shaly caprock at atmospheric temperature. Their main results show that the effects induced by the presence of CO<sub>2</sub> as a non-wetting fluid must be carefully considered; reduction of the interfacial tension and the possible variation in contact angle. These aspects were found to cause a reduction of the entry pressure in the presence of CO<sub>2</sub>.

Farokhpour et al. [14] were targeting to present a project about the possible changes in wettability due to physical-geochemical processes which could decrease the capillary entrance pressure and reduce the sealing integrity of the caprock. Their results showed that exposing muscovite mica mineral to CO<sub>2</sub> showed a marked increase in contact angle and minerals became significantly less water wet. Also, capillary entry pressure measurements resulted in reduction in capillary entry pressure. The permeability measurements after each test showed significant change in shale absolute permeability to brine.

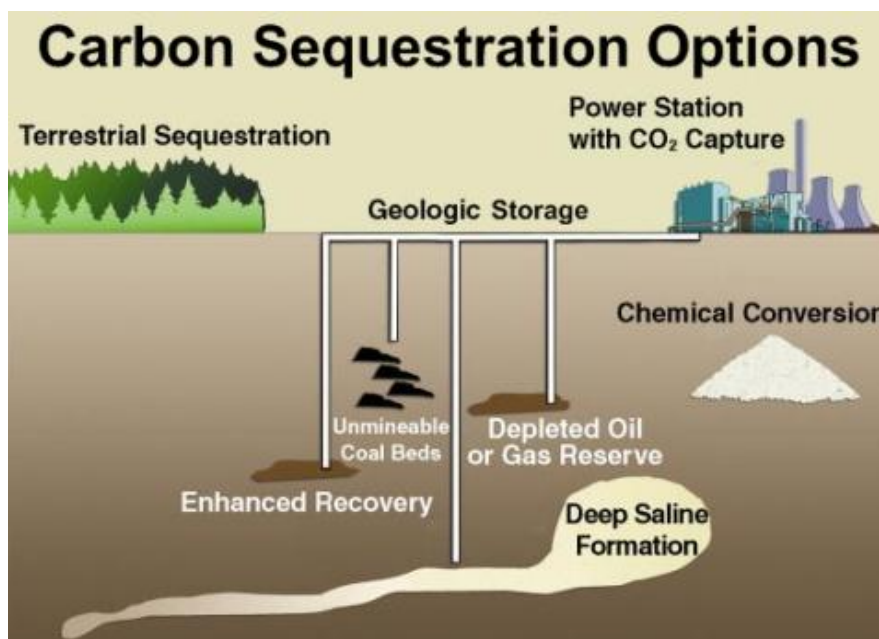


**Fig. 1. Carbon geological storage, where the CO<sub>2</sub> is injected and stored in high permeability and porosity formation with overlying caprock [6]**

Pini et al. [15] used sandstones rock cores with different lithology and pore size distribution to measure drainage capillary pressure curves of CO<sub>2</sub> and water. They noticed that these measurements provide independent confirmation

that sub-core scale capillary heterogeneity plays an important role in controlling saturation distributions during multiphase flow. Comisky et al. [16] measured mercury injection capillary pressure (MICP) profiles on tight shale samples

with a variety of sample sizes. MICP profiles show a very strong dependence on sample size due to two reasons: pore accessibility and conformance. Cuttings and core profiles for use in calibrating well logs have proven to be a requirement in ultra-low perm systems. AL-Bazali et al. [17] focused on proving that the shale properties (CEC and permeability), fluid type, and interfacial tension can make a difference in the values of capillary entry pressures of shales at atmospheric temperature ( $T= 70^{\circ}\text{F}$ ). Their data showed that as the value of interfacial tension increases, the capillary entry pressure increases, the relationship between the capillary entry pressure and shale permeability is an inverse relationship, and shales with high CEC exhibited high capillary breakthrough pressure.

Abdoulghafour et al. [18] targeted measuring capillary pressure curves as a function of water saturation, saturation history, rock matrix, and thermo-physical conditions. Sandstone samples showed that the  $\text{CO}_2$  saturation increased with increasing  $\text{CO}_2$  injection rate, typical for a non-wetting phase displacement. There was also a clear increase in the Saturation of  $\text{CO}_2$  with increasing  $P_c$ . Plug & Bruining [19] investigated capillary pressure for the sand- $\text{CO}_2$ -water system under various pressure conditions at the atmospheric temperature ( $T= 27^{\circ}\text{C}$ ). Their experimental results show a decrease of drainage and imbibition capillary pressure for increasing  $\text{CO}_2$  pressures and pronounced dissolution rate effects for gaseous  $\text{CO}_2$ . Significant capillary pressure fluctuations and negative values during imbibition are observed at near critical conditions.

Dewhurst et al. [20] investigated, using drying method, threshold pressure determinations for the Muderong shale and indicated that for such a stiff, cemented shale, method of drying does not significantly influence determination of threshold pressure. The measured capillary properties of Muderong Shale indicate that, given a lack of other seal risk factors, it is liable to form an excellent sealing lithology to hydrocarbons and for the geological sequestration of  $\text{CO}_2$ . Also, compositional variations through Muderong Shale sequence, especially increasing smectite interlayer content in illite-smectite lower in the sequence in the deeper basin, would likely increase seal capacity.

Donnelly et al. [21] studied capillary pressure - saturation relationships for gas shales measured using a water activity meter. As expected, the different shale types had statistically different Brooks and Corey parameters. However, there

were no significant differences between the Brooks and Corey parameters for the wetting and drying measurements, suggesting that hysteresis may not need to be considered in leak off simulations.

Olabode & Radonjic [22] investigated the caprock integrity in  $\text{CO}_2$  sequestration in their study. Their results showed that rock properties of shale can be significantly altered by minute geochemical changes that are hard to detect. These geochemical changes affect the specific surface area and pore network of shale caprock such that in all the samples examined, their values tended to increase with time though at reduced rates in the later time of the experiment. Chenevert & Amanullah [23] discussed results obtained with a specially preserved, highly reactive shale core. This study showed that shales must be preserved at their native water content if accurate physical measurements are to be made. The data of swelling revealed that shales that were altered during handling (hydrated or dehydrated) did not respond properly even when restored to their native hydration conditions and experienced excessive swelling compared to cores kept at their native water content.

Hale et al. [24] analyzed the influence of chemical potential on wellbore stability. Their results are explained based on chemical potential differences between oil-based drilling fluid and shale. The change in shale water content caused by these differences is identified as the predominant factor leading to alteration of shale mechanical behavior and hence borehole stability. A review of geological applications and interpretations of capillary pressure in reservoir studies had been presented by [25]. They evaluated seal potential of shale caprocks and presented important equations that can help estimating the shale sealing capacity and reservoir versus non-reservoir or pay versus non-pay zones in details.

Some new models and methodologies have been proposed which can be useful such as [26], [27] where they developed a new ET model for prediction of ( $B_o$  and  $P_b$ ) using only two parameters ( $R_{si}$  and  $\gamma_g$ ). The developed models exhibit strong performance and comparably accurate predictions. Mathias et al. [28] developed a two-layer vertical equilibrium model for the injection of carbon dioxide into a low-pressure porous reservoir containing methane and water. Their results showed that as the initial pressure in the reservoir decreases, both the pressure buildup and temperature change increase. Zendehboudi et al. [29] proposed a

new methodology for the acceleration of CO<sub>2</sub> dissolution to lower the risk of CO<sub>2</sub> leakage for carbon capture and storage (CCS) technology. This new approach reduces or eliminates possible leakage of CO<sub>2</sub> from underground formation.

Bennion & Bachu [30] studied permeability and relative permeability at reservoir conditions for CO<sub>2</sub>-Water systems for different caprocks. They found that any appreciable losses of CO<sub>2</sub> over a non-geological time scale would be minimal to non-existent. Burnside & Naylor [31] discussed the geological trapping mechanisms, which can guarantee immobilization of CO<sub>2</sub> in the reservoir, even in the event of leakage. They found that all of the shale samples and all but three of the carbonate samples have low  $K_r^{CO_2}$  values (<0.2). The main goal of [32] work is to minimize the fraction of cumulatively produced CO<sub>2</sub> to cumulatively produced oil. According to their results of several simulations and optimizations and compared to reservoir history, amounts of stored CO<sub>2</sub>, and recovered oil increased, for a real geological formation. Ziaabakhsh-Ganji & Kooi [33] investigated the impact of presence of other gases (impurities) in the injected CO<sub>2</sub> stream on Joule–Thomson cooling. Their main results showed that presence of gases (impurities) affect both the spatial extent of the zone around the wellbore in which cooling occurs and the magnitude of cooling. Paterson et al. [34] did an observation regarding thermal and pressure transients in carbon dioxide wells. Injection of carbon dioxide - rich gases can cause substantial cooling of the reservoir close to the injection point. The effect of this cooling on reservoir properties needs further investigation.

After investigating these previous studies which provided an insight on the shale sealing capacity, it has been noticed that most of these studies were conducted under ambient temperature which does not represent in-situ conditions. Also, these studies ignored the impact of temperature on the physical properties of interacting fluids, petrophysical properties of shale such as permeability and porosity, and physicochemical properties of shale such as clay swelling, water activity and water content. Shale sealing ability can be affected by the thermal changes in physical and chemical properties of shale and CO<sub>2</sub>.

In this study, changes in capillary entry pressure of carbon dioxide when interacting with shale under different range of temperatures (25°C to 250°C) have been investigated. The impact of temperature on the physicochemical and petrophysical properties of shale is also

addressed. In addition, the influence of temperature on the interfacial tension between CO<sub>2</sub> and shale pore fluid, contact angle, and pore throat radius is examined. Understanding all these effects may lead to a better evaluation of the shale ability to sequester CO<sub>2</sub>. Carbene dioxide (CO<sub>2</sub>) sequestration in shale formations projects may be compromised, if the impact of temperature is completely ignored.

### 3. SHALE SAMPLES PROPERTIES

In this project, three shale types, shales A, B & C, were investigated. Shales A, B & C have been donated by an oil company in Kuwait for research purposes. When shale cores arrived at Kuwait University, they were coated and covered in a thick polyethylene bag and well-preserved in a closed barrel. This handling procedure avoids shale pore structure contamination by air since air penetration could cause shale properties alteration.

To avoid shale damage such as microfractures, fissures and cracks, the polyethylene bag was carefully removed, and the shale cores were immediately uncovered and entirely immersed in cans full of mineral oil. The immersion of shale cores in mineral oil prevents air interaction with shale and preserve its native water content and water activity [35]. The petrophysical properties and mineralogical composition of shales A, B & C are shown in Tables 1 & 2, respectively.

### 4. EXPERIMENTAL METHODOLOGY

The purpose of this test is to measure the capillary entry pressure of shale when interacting with CO<sub>2</sub> under variant temperatures. Fig. 2 shows the experimental set up and equipment used for the minimum capillary entry pressure test. The equipment and experimental set up shown in Fig. 2 are fitted inside a heavy-duty oven so temperature can be changed as needed.

Shale sample is positioned inside the main cell. Carbene dioxide (CO<sub>2</sub>) is placed in the top chamber vessel where a pressure regulator is used to regulate the pressure of injected CO<sub>2</sub>. The bottom chamber of the vessel is connected to a CO<sub>2</sub> cylinder. A flow line is connected between the main cell and the top chamber of the pressure vessel so that CO<sub>2</sub> can flow into the shale. A pressure gauge is placed in the flow line to monitor the pressure of CO<sub>2</sub>. A valve is also placed in the flow line to bleed the CO<sub>2</sub> once the test is terminated. On the other side of the main cell, a volume chamber was connected to the bottom of the cell. Using an injection pump, this chamber is filled with a simulated pore fluid and pressurized to 50 psi. A pressure gauge is connected to this chamber to monitor pressure

changes in this chamber. The following steps are taking to measure the capillary entry pressure of CO<sub>2</sub> through shale:

- Insert the shale sample in the main cell which is situated inside the oven and set the temperature of the oven to the desired temperature.
- Using the injection pump, the downstream chamber is filled with simulated pore fluid and pressurized to 50 psi. Using a simulated pore fluid prevents water exchange between shale and the downstream chamber by chemical osmosis means.
- Fill the top compartment of the pressure chamber, connected to the CO<sub>2</sub> cylinder, with CO<sub>2</sub>.
- Open the CO<sub>2</sub> cylinder by opening the valve above it allowing CO<sub>2</sub> to flow through the bottom compartment thereby forcing the piston to push the CO<sub>2</sub> in the top compartment through the shale.
- The flowing CO<sub>2</sub> pressure is monitored through pressure transducer 2 while the simulated pore pressure in the downstream chamber is monitored through pressure transducer 1.
- If the simulated pore pressure in the downstream chamber did not change, increase the CO<sub>2</sub> flowing pressure by allowing more volume of CO<sub>2</sub> to flow from the CO<sub>2</sub> cylinder.
- Once a pressure change is detected in the downstream chamber (transducer 1), the test is terminated and the pressure reading on pressure transducer 2 reflects the capillary entry pressure of CO<sub>2</sub> through shale sample at the set temperature.
- Change the temperature of the oven to a different value and repeat the test to obtain the capillary entry pressure of CO<sub>2</sub> through shale at the new temperature. Full description of the experimental procedure can be found in [9].

**Table 1. Petrophysical properties of shales A, B and C**

	<b>Water Content (%)</b>	<b>Water Activity</b>	<b>Porosity (%)</b>	<b>Permeability (nD)</b>
Shale (A)	5.9	0.91	15.3	3.1
Shale (B)	6.1	0.86	13.8	1.3
Shale (C)	5.8	0.89	14.7	2.7

**Table 2. Mineralogical composition of shales A, B and C**

<b>X-Ray Diffraction</b>	<b>Shale (A) % by Weight</b>	<b>Shale (B) % by Weight</b>	<b>Shale (C) % by Weight</b>
Quartz	17	23	19.8
Feldspar	3.8	3.9	4
Calcite	2.9	0	1.9
Dolomite	7.5	1.6	3.1
Pyrite	2.3	1.9	2
Siderite	1.1	3.7	3.5
Total Clay	64.1	64.5	68.5
<i>Chlorite</i>	3.1	2.9	3.2
<i>Kaolinite</i>	6.4	5.5	6.1
<i>Illite</i>	11.8	15	14.8
<i>Smectite</i>	11.5	11.7	12.1
<i>Mixed Layer</i>	31.3	29.4	32.3

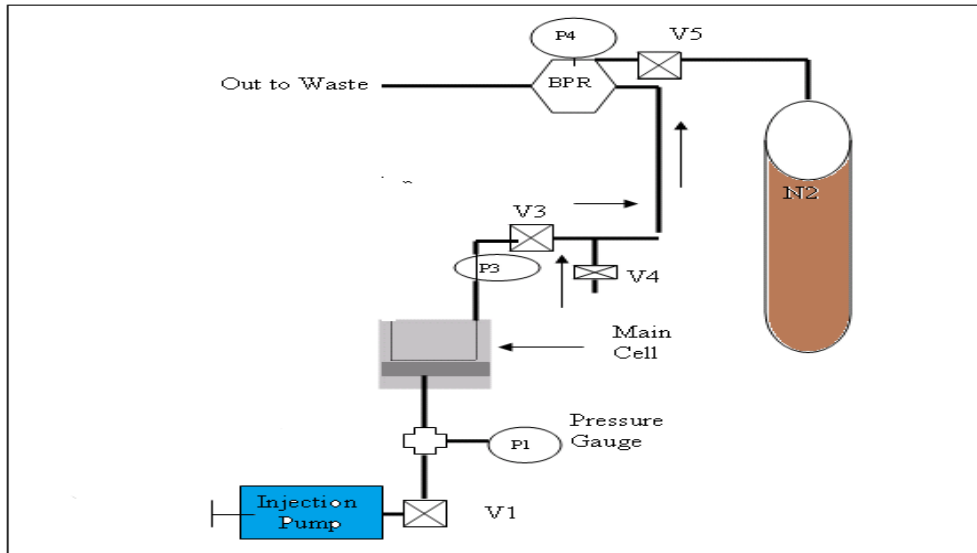


Fig. 2. Experimental set up and equipment used for capillary entry pressure test

## 5. RESULTS AND DISCUSSION

### 5.1 General Analysis of Capillary Entry Pressure When Shale Interacts with CO<sub>2</sub>

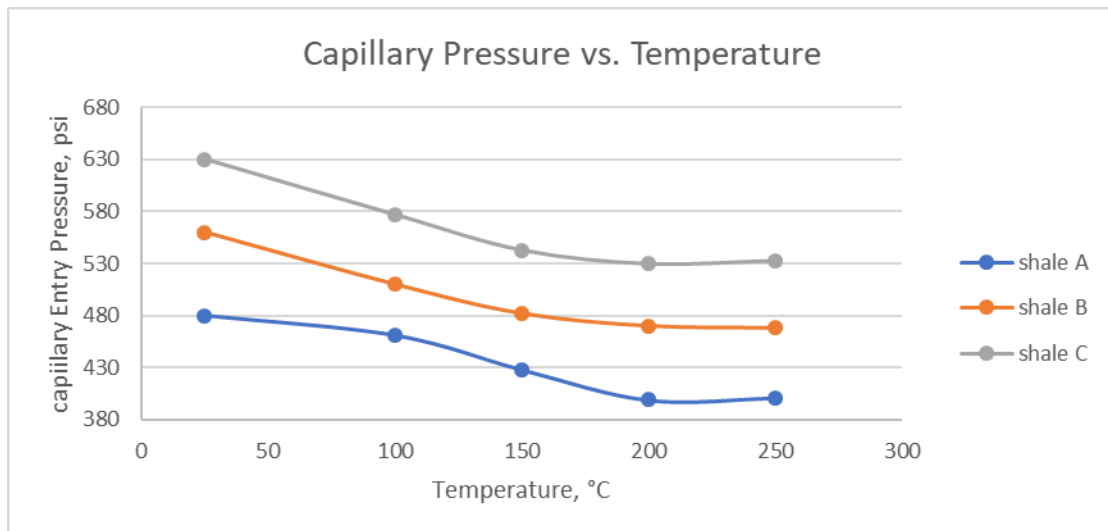
Table 3 and Fig. 3 show experimental results of capillary entry pressure measurements when three different shales interacted with CO<sub>2</sub> at variant temperatures (25°C – 250°C).

It can be observed, in Fig. 3, that there is a difference in the capillary entry pressure values of shales A, B and C where shale A has the lowest values of capillary entry pressure and shale C has the largest values of capillary entry

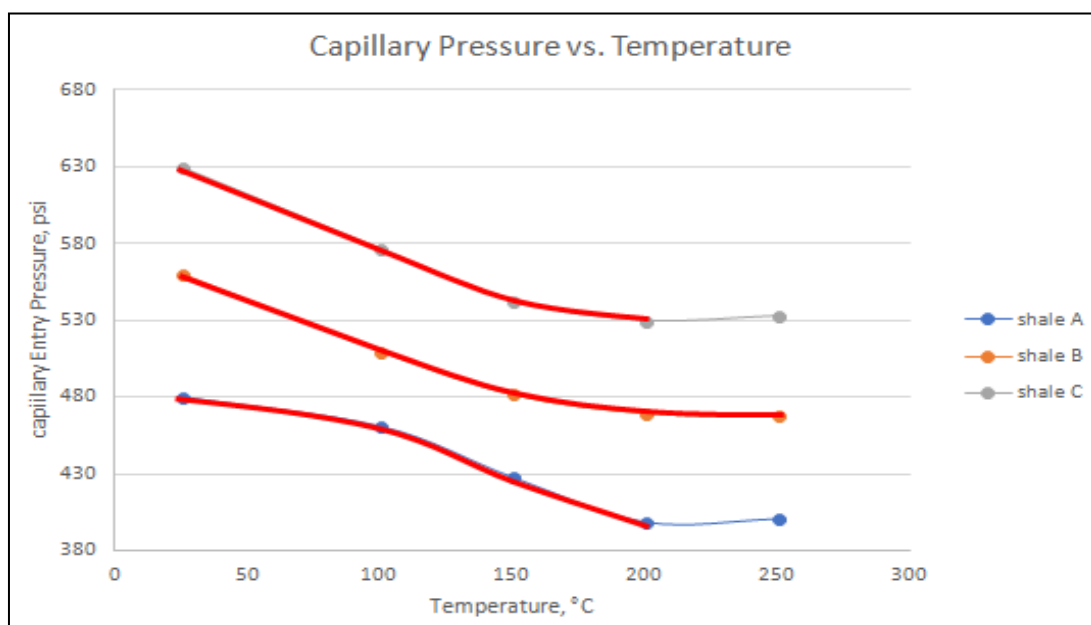
pressure. There are many parameters that can affect the capillary entry pressure of shale such as chemical composition, petro-physical properties, wettability, fluid properties (interfacial tension and contact angle), density differences between fluid pairs and formation saturation history [36]. The difference in capillary entry pressure can be attributed to the differences in these parameters for each shale. It can also be seen, in Fig. 4, that the values of capillary pressure for shales A and C decreased until 200°C, after which it increased slightly. However, the values of capillary entry pressure for shale B decreased for all temperatures.

Table 3. Capillary pressure measurements for shales A, B & C at different temperatures

Temperature (°C)	Shale A (Pc), psi	Shale B (Pc), psi	Shale C (Pc), psi
25	480	560	630
100	461	510	577
150	428	482	543
200	399	470	530
250	401	468	533



**Fig. 3. Capillary entry pressure for shales A, B and C at variant temperatures**



**Fig. 4. Capillary entry pressure for shales A and C vs. shale B at variant temperatures**

According to equation 1, capillary entry pressure depends on three factors; interfacial tension ( $\sigma$ ), contact angle ( $\theta$ ), and shale pore throat radius ( $r$ ). It is clear that capillary entry pressure is inversely proportional to pore throat radius ( $r$ ) where an increase in ( $r$ ) will cause a decrease in capillary entry pressure of shale. It can be argued that increasing temperature may have caused pore dilation. Pore dilation is scientifically defined as the enlarging, expanding, or widening of pores which will cause an increase in the pore throat radius of shale [37].

The second parameter that must be discussed is interfacial tension which is directly proportional to capillary entry pressure. When the value of interfacial tension decreases, the value of

capillary entry pressure will decrease and vice versa. It has been stated that increasing temperature will affect interfacial tension between two immiscible fluids [38], [39-41]. These studies, among others, have shown that an increase of temperature decreases the interfacial tension between two immiscible fluids owing to the weakening of intermolecular forces at the two immiscible fluids interface. It follows, according to equation 1, that a decrease in interfacial tension between two immiscible fluids, will cause a decrease in capillary entry pressure developed at their interface.

The third parameter that needs to be investigated is the contact "wettability" angle. As found in the literature, there was a discrepancy between

studies regarding wettability angle ( $\Theta$ ) where some studies found that ( $\Theta$ ) would increase with temperature [42] and other studies found that wettability angle ( $\Theta$ ) would decrease with increasing temperature [43], [44], [45]. This discrepancy may be attributed to differences in salt concentration, salt type, or surface roughness. This shows that the contact “wettability” angle may increase or decrease with temperature depending on the parameters involved. We believe that the combined effect of wettability angle and interfacial tension may have caused a decrease in capillary entry pressure of shale.

It can also be observed, in Fig. 5, that the values of capillary entry pressures at 250°C increased in shales A and C and decreased for shale B. A closer look at the mineralogical composition for the three shales indicates that this increase is due to shale swelling owing to fact that shales A and C contain larger amounts of swelling clay (smectite and mixed layers) than shale B. Smectite and mixed layers clays are highly swelling clays containing high amount of montmorillonite clay which causes water adsorption and subsequent clay swelling. Generally, clays are divided into two types: macroscopically swelling, ‘active’ clays, and ‘passive’ or non-swelling clays. According to [46], [47], [48], [49] temperature could induce a transition that turns passive non-swelling clay to active swelling clay. While net attractive forces are dominant at low temperatures so that the clay particles remain attached to each other in stacks, at higher temperatures it is energetically favorable for the clay to swell due to the entropy gained by counterions which are liberated during swelling.

The sum of smectite and mixed layers ‘active clays’ in shales A, B, and C were found to be 42.8, 41.1, and 44.4 %by weight, respectively. Shale B has the lowest amount of swelling “active” clay, which could explain why the capillary pressure did not increase at 250 °C. This could be due to the fact that the amount of active clay was not enough to cause shale swelling at 250 °C. The increase in capillary entry pressure for shale C was higher than that for shale A at 250 °C. This may be attributed to the larger amount of active swelling clay in shale C than in shale A. Clay swelling may cause an apparent decrease in pore throat radii of shale which translates into higher capillary entry pressure, according to equation 1, as CO<sub>2</sub> interacts with shale.

## 5.2 Impact of Water Content (w%) on Capillary Entry Pressure

Fig. 6 shows measured capillary entry pressure versus water content of shale as a function of temperature. Water content is defined as the ratio of the weight of water to the weight of the solids for a given mass of material and is usually expressed as percentage [50]. It is clear that there exists no distinct relationship between shale water content and the expected capillary entry pressure as shale interacts with CO<sub>2</sub>. The impact of water content may be levied within other factors such as pore throat radii. Green et al., 2008 argue that capillary entry pressure of shale caprocks decreases with increasing water content of shale due to the spontaneous imbibition of water. Due to imbibition, the increase in water saturation causes an increase in its relative permeability and in turn decrease in capillary pressure since the capillary pressure is inversely proportional to relative permeability [51].

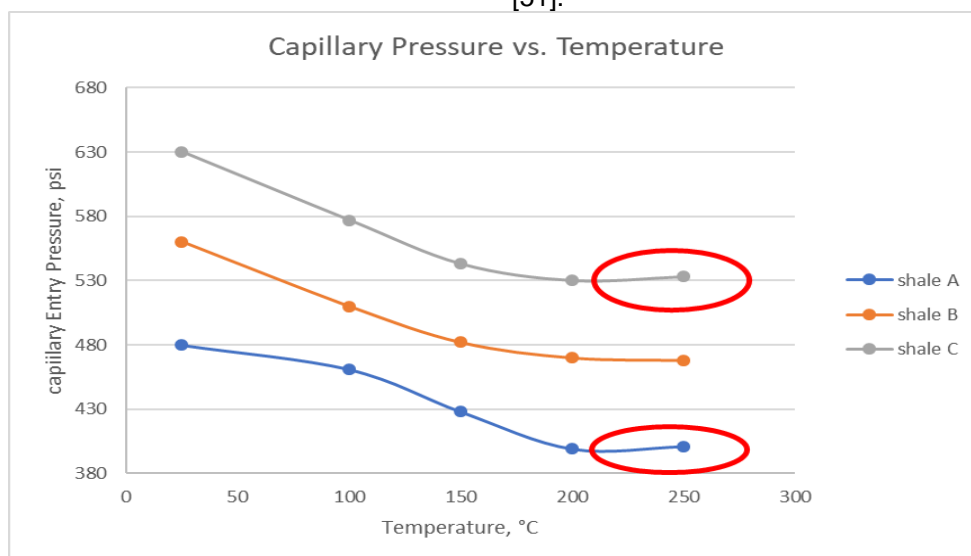


**Fig. 5. A look at capillary entry pressure for shales A, B and C at 250°C**

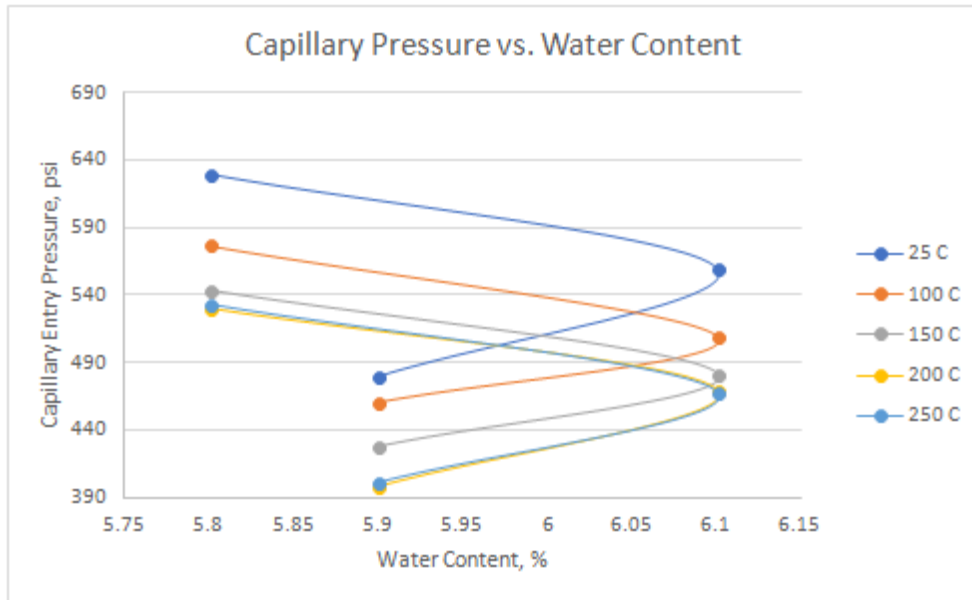


**Fig. 6. Measured capillary entry pressure versus water content of shale as a function of temperature**

### 5.3 Impact of Water Activity ( $a_w$ ) on Capillary Entry Pressure

By definition, water activity ( $a_w$ ) is the ratio of the vapor pressure of water in a material to the vapor pressure of pure water at the same temperature [52]. Fig. 7 shows measured capillary entry pressure as a function of shale water activity as shale interacts with  $CO_2$  at different temperatures. Same as water content, there is no consistent relationship between shale water activity and measured capillary entry pressure

and this could be attributed to the mineralogical and chemical composition of shale. Generally speaking, it can be clearly seen that the measured capillary entry pressure decreases as temperature decreases regardless of the shale water activity. This leads me to believe that the impact of water activity on capillary entry pressure of shale is secondary as other primary factors such as interfacial tension, pore throat radii and wettability angle play a more dominant role as discussed in section 6.1.

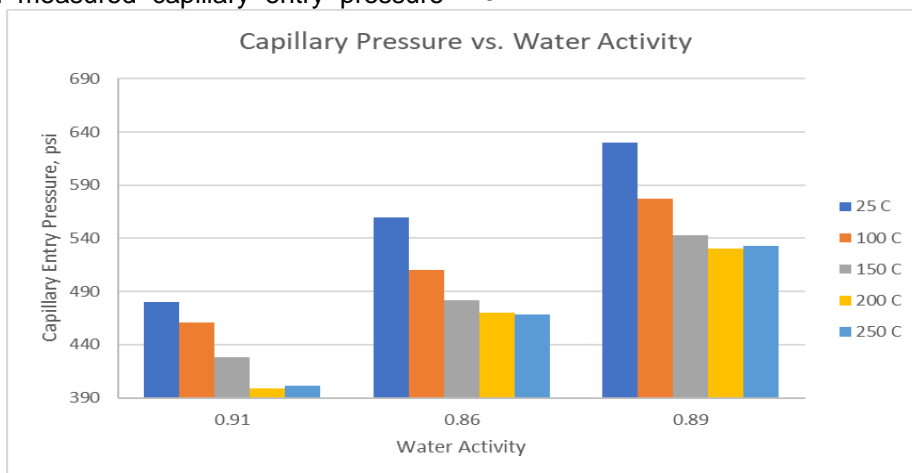


**Fig. 7. Measured capillary entry pressure versus water activity of shale as a function of temperature**

### 5.4 Impact of Shale Permeability on Capillary Entry Pressure

Shale's permeability is described by an average pore throat radius of the shale's pores. The average shale's pore radius can be changed to shale's permeability using the following equation:

$$k = \frac{\phi r^2}{8} \tag{3}$$

From equation (1), it can be concluded that pore radius is inversely proportional to capillary entry pressure. This means that low permeability shales should record higher capillary entry pressures than high permeability shales. This did not happen consistently in our experiments as shown in Fig. 8. In Fig. 8, shale C (k = 2.7 nD) had higher capillary entry pressure than shale B (k = 1.3 nD) at all applied temperatures. This is counter intuitive and could be related to the effect of temperature on pore throat radii size and structure. Pore throat radii may have experienced pore dilation upon exposure to heat and this may have caused changes in pore throat radii sizes. It is argued that pore throat size could be altered by heat through a phenomenon called 'pore dilation'. It is possible that different shales respond to heat differently depending on the shale texture, fabric and pore network structure and mineralogical composition. Therefore, higher temperatures could have changed the mechanical structure of shale by impacting its pore throat size and distribution. Consequently, excessive heat could have affected the size of the largest pore throat of shale which may have caused lower than expected capillary entry pressures for shale B.

Measured capillary entry pressures for shale A (k = 3.1 nD) came in expectation and agreement with equations (1 & 3). Shale A had the highest permeability and in turn would have the highest pore throat radii and should record the lowest capillary entry pressure as seen in Table 3.

### 5.5 Impact of Shale Porosity on Capillary Entry Pressure

The porosities of shales A, B and C correlate very well with their permeabilities as shown in Table 4.

**Table 4. Porosities and permeabilities of shales A, B and C**

	Porosity (%)	Permeability (nD)
Shale A	15.3	3.1
Shale B	13.8	1.3
Shale C	14.7	2.7

On average, low permeability rocks should have smaller pore throat radii and thus should exhibit higher capillary entry pressure. Our data did not follow this argument precisely because shale B (f = 13.8%) showed lower capillary entry pressure than shale C (f = 14.7%). Shale A (f = 15.3%) seems to agree with our expectations.

We could use the same argument that we used in section 6.4 where heat could have altered the pore throat radii and caused pore dilation. Shales A, B and C pore structure responded differently to the application of heat depending on each shale fabric, texture and mechanical properties. This pore dilation may have been responsible for the discrepancy of measured capillary entry pressure.

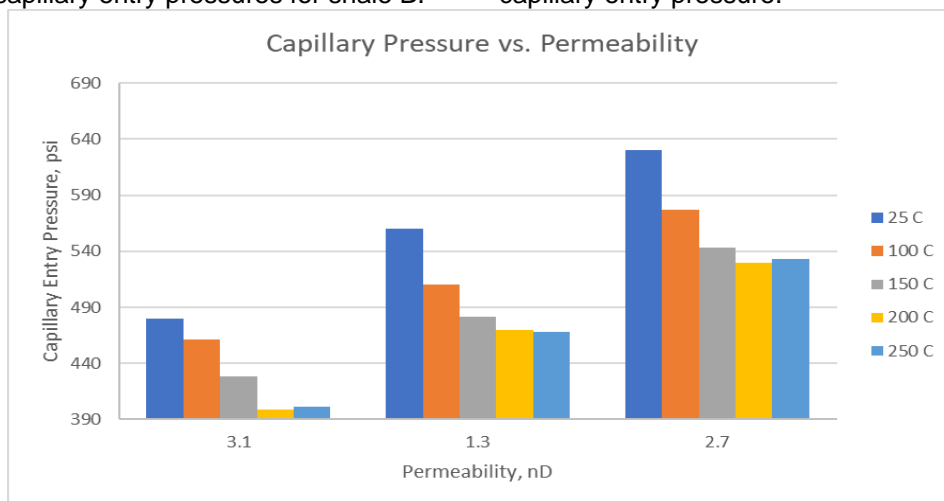


**Fig. 8. Measured capillary entry pressure versus permeability of shale as a function of temperature**

## 6. CONCLUSIONS AND RECOMMENDATIONS

The following conclusions and recommendations were drawn from this work:

- Difference in the capillary entry pressure values of shales A, B and C, can be attributed, to the differences in petrophysical properties, chemical composition, wettability, fluid properties (interfacial tension and contact angle), density differences between fluid pairs and formation saturation history for each shale.
- The capillary entry pressure of shales A and C decreased until 200 °C, after which it increased slightly.
- The values of capillary entry pressure for shale B decreased at all temperatures.
- The capillary entry pressure values depend on three factors; interfacial tension ( $\sigma$ ), contact angle ( $\theta$ ), and shale pore throat radius ( $r$ ).
- It is clear that capillary entry pressure is inversely proportional to pore throat radius  $r$ , which means an increase in  $r$  will cause a decrease in  $P_c$  value.
- With temperature increasing, pores are exposed to a phenomenon called pore dilation. Pore dilation means the action of enlarging, expanding, or widening of pores which will cause an increase in the pore throat radius  $r$ .
- Interfacial tension is linearly proportional to capillary entry pressure, so that when interfacial tension decreases the value of capillary entry pressure will decrease and vice versa.
- Interfacial tension decreases with increasing temperature and that can be attributed to the weakening of intermolecular forces at the two immiscible fluids interface.
- Wettability angle discrepancy may be attributed to differences in, salt concentration, salt type, or surface roughness.
- At 250 °C, capillary entry pressure increased for shales A and C which may be attributed to the swelling of clay minerals.
- Swelling of clay could be related to temperature-induced transition from passive to an active clay.
- The amount of swelling clay in shale C was higher than in shale A which could explain why the increase of capillary entry pressure at 250°C in shale C was higher than shale A.

- It is clear that there exists no distinct relationship between shale water content and water activity, and the expected capillary entry pressure as shale interacts with CO<sub>2</sub>.
- Heat could alter the pore throat radii and cause pore dilation. This pore dilation may have been responsible for the discrepancy of measured capillary entry pressure.
- Shales A, B and C pore structure responded differently to the application of heat depending on each shale fabric, texture and mechanical properties.
- It is recommended to use different kind of caprocks instead of shales like carbonate caprocks.
- It is recommended to elevate pressure with elevating temperature to investigate the effect of increasing pressure and temperature together, in-situ condition.

## COMPETING INTERESTS

Authors have declared that no competing interests exist.

## REFERENCES

1. Qiao Z, Wang Z, Zhang C, Yuan S, Zhu Y, Wang J. PVAm-PIP/PS composite membrane with high performance for CO<sub>2</sub>/N<sub>2</sub> separation. *AIChE Journal*. 2012; 59(4):215–228. Available: <https://doi.org/10.1002/aic>.
2. Shukla R, Ranjith P, Haque A, Choi X. A review of studies on CO<sub>2</sub> sequestration and caprock integrity. *Fuel*. 2010;89(10):2651–2664. Available: <https://doi.org/10.1016/j.fuel.2010.05.012>.
3. Benson SM, Cole DR. CO<sub>2</sub> sequestration in deep sedimentary formations. *Elements*. 2008;4(5):325–331. Available: <https://doi.org/10.2113/gselements.4.5.325>.
4. Broadhead R. *Petroleum Geology: an Introduction*. New Mexico Bureau of Geology and Mineral Resources; 2002.
5. Traps P. Gas Oil. *Encyclopedia of Lubricants and Lubrication*. 2014;727–727. Available: [https://doi.org/10.1007/978-3-642-22647-2\\_200181](https://doi.org/10.1007/978-3-642-22647-2_200181).
6. Espinoza DN, Santamarina JC. CO<sub>2</sub> breakthrough—Caprock sealing efficiency and integrity for carbon geological storage. *International Journal of Greenhouse Gas Control*. 2017a;66:218–229. Available: <https://doi.org/10.1016/j.ijggc.2017.09.019>.

7. Jennings JB. Capillary Pressure techniques: Application to exploration and development geology. American association of petroleum geologists bulletin. 1987;71(10):1196–1209. Available:<https://doi.org/10.1306/703c8047-1707-11d7-8645000102c1865d>.
8. Egermann P, Lombard JM, Bretonnier P. A fast and accurate method to measure threshold capillary pressure of caprocks under representative conditions. *Sca*, 2006;1–14.
9. Al-Bazali TM, Zhang J, Chenevert ME, Sharma MM. Estimating the reservoir hydrocarbon capacity through measurement of the minimum capillary entry pressure of shale caprocks. In SPE Annual Technical Conference and Exhibition. One Petro; 2009.
10. Chang YB, Lim MT, Pope GA, Sepehrnoori K. CO<sub>2</sub> flow patterns under multiphase flow: Heterogeneous field-scale conditions. SPE Reprint Series. 1999;51:145–153.
11. Espinoza DN, Santamarina JC. CO<sub>2</sub> breakthrough—Caprock sealing efficiency and integrity for carbon geological storage. *International Journal of Greenhouse Gas Control*. 2017b ;66:218–229. Available:<https://doi.org/10.1016/j.ijggc.2017.09.019>.
12. Berg RR. Capillary Pressures in Stratigraphic Traps. AAPG Bulletin (American Association of Petroleum Geologists). 1975;59(6):939–956. Available:<https://doi.org/10.1306/83d91ef7-16c7-11d7-8645000102c1865d>.
13. Favero V, Laloui L. Impact of CO<sub>2</sub> injection on the hydro-mechanical behaviour of a clay-rich caprock. *International Journal of Greenhouse Gas Control*. 2018;71:133–141. Available:<https://doi.org/10.1016/j.ijggc.2018.02.017>.
14. Farokhpour R, Bjørkvik BJA, Lindeberg E, Torsæter O. Wettability behaviour of CO<sub>2</sub> at storage conditions. *International Journal of Greenhouse Gas Control*. 2013b;12:18–25. Available:<https://doi.org/10.1016/j.ijggc.2012.11.003>.
15. Pini R, Krevor SCM, Benson SM. Capillary pressure and heterogeneity for the CO<sub>2</sub>/water system in sandstone rocks at reservoir conditions. *Advances in Water Resources*. 2012;38:48–59. Available:<https://doi.org/10.1016/j.advwatres.2011.12.007>.
16. Comisky JT, Santiago M, McCollom B, Buddhala A, Newsham KE. Sample size effects on the application of mercury injection capillary pressure for determining the storage capacity of tight gas and oil shales. Society of Petroleum Engineers - Canadian Unconventional Resources Conference 2011, CURC. 2011;3(1992): 2103–2125. Available:<https://doi.org/10.2118/149432-ms>.
17. Al-Bazali T, Zhang J, Chenevert ME, Sharma MM. Maintaining the stability of deviated and horizontal wells: Effects of mechanical, chemical and thermal phenomena on well designs. *Geomechanics and Geoengineering: An International Journal*. 2008;3(3):167–178.
18. Abdoulghafour H, Sarmaadivaleh M, Hauge LP, Fernø M, Iglaue S. Capillary pressure characteristics of CO<sub>2</sub>-brine-sandstone systems. *International Journal of Greenhouse Gas Control*. 2020;94: 102876. Available:<https://doi.org/10.1016/j.ijggc.2019.102876>.
19. Plug WJ, Bruining J. Capillary pressure for the sand-CO<sub>2</sub>-water system under various pressure conditions. Application to CO<sub>2</sub> sequestration. *Advances in Water Resources*. 2007;30(11):2339–2353. Available:<https://doi.org/10.1016/j.advwatres.2007.05.010>.
20. Dewhurst DN, Jones RM, Raven MD. Microstructural and petrophysical characterization of Muderong Shale: Application to top seal risking. *Petroleum Geoscience*. 2002;8(4):371–383. Available:<https://doi.org/10.1144/petgeo.8.4.371>.
21. Donnelly B, Perfect E, McKay LD, Lemiszki PJ, DiStefano VH, Anovitz LM, McFarlane J, Hale RE, Cheng CL. Capillary pressure – saturation relationships for gas shales measured using a water activity meter. *Journal of Natural Gas Science and Engineering*. 2016;33:1342–1352. Available:<https://doi.org/10.1016/j.jngse.2016.05.014>.
22. Al-Bazali TM, Zhang J, Wolfe C, Chenevert ME, Sharma MM. Wellbore instability of directional wells in laminated and naturally fractured shales. *Journal of Porous Media*. 2009;12(2).
23. Chenevert ME, Amanullah M. Shale preservation and testing techniques for borehole-stability studies. *SPE Drilling and Completion*. 2001;16(3):146–149. Available:<https://doi.org/10.2118/73191-PA>.

24. Hale AH, Mody FK, Salisbury DP. Influence of chemical potential on wellbore stability. *SPE Drilling and Completion*. 1993;8(3):207–216. Available: <https://doi.org/10.2118/23885-PA>.
25. Vavra CL, Kaldi JG, Sneider RM. Geological applications of capillary pressure: A review. *American Association of Petroleum Geologists Bulletin*. 1992; 76(6):840–850. Available: <https://doi.org/10.1306/bdff88f8-1718-11d7-8645000102c1865d>.
26. Seyyedattar M, Ghiasi MM, Zendehboudi S, Butt S. Determination of bubble point pressure and oil formation volume factor: Extra trees compared with LSSVM-CSA hybrid and ANFIS models. *Fuel*. 2020; 269:116834. Available: <https://doi.org/10.1016/j.fuel.2019.116834>.
27. Busch A, Alles S, Gensterblum Y, Prinz D, Dewhurst DN, Raven MD, Stanjek H, Krooss BM. Carbon dioxide storage potential of shales. *International Journal of Greenhouse Gas Control*, 2008;2(3):297–308. Available: <https://doi.org/10.1016/j.ijggc.2008.03.003>.
28. Mathias SA, McElwaine JN, Gluyas JG. Heat transport and pressure buildup during carbon dioxide injection into depleted gas reservoirs. *Journal of Fluid Mechanics*. 2014;756:89–109. Available: <https://doi.org/10.1017/jfm.2014.348>.
29. Zendehboudi S, Khan A, Carlisle S, Leonenko Y. Ex situ dissolution of CO<sub>2</sub>: A new engineering methodology based on mass-transfer perspective for enhancement of CO<sub>2</sub> sequestration. *Energy and Fuels*. 2011;25(7):3323–3333. Available: <https://doi.org/10.1021/ef200199r>.
30. Bennion DB, Bachu S. Permeability and relative permeability measurements at reservoir conditions for CO<sub>2</sub>-water systems in ultra low permeability confining caprocks. 69th European Association of Geoscientists and Engineers Conference and Exhibition 2007: Securing The Future. Incorporating SPE EUROPEC. 2007; 1:401–410. Available: <https://doi.org/10.2523/106995-ms>.
31. Burnside NM, Naylor M. Review and implications of relative permeability of CO<sub>2</sub>/brine systems and residual trapping of CO<sub>2</sub>. *International Journal of Greenhouse Gas Control*. 2014;23:1–11. Available: <https://doi.org/10.1016/j.ijggc.2014.01.013>.
32. Eshraghi SE, Rasaei MR, Zendehboudi S. Optimization of miscible CO<sub>2</sub> EOR and storage using heuristic methods combined with capacitance/resistance and Gentil fractional flow models. *Journal of Natural Gas Science and Engineering*. 2016;32: 304–318. Available: <https://doi.org/10.1016/j.jngse.2016.04.012>.
33. Ziabakhsh-Ganji Z, Kooi H. Sensitivity of Joule-Thomson cooling to impure CO<sub>2</sub> injection in depleted gas reservoirs. *Applied Energy*, 2014;113:434–451. Available: <https://doi.org/10.1016/j.apenergy.2013.07.059>.
34. Al-Bazali TM, Zhang J, Chenevert ME, Sharma MM. An experimental investigation on the impact of diffusion osmosis, chemical osmosis, and capillary suction on shale alteration. *Journal of Porous Media*. 2008;11(8).
35. Al-Bazali T, Zhang J, Chenevert ME, Sharma MM. Experimental and numerical study on the impact of strain rate on failure characteristics of shales. *Journal of Petroleum Science and Engineering*. 2008; 60(3-4):194-204.
36. McPhee C, Reed J, Zubizarreta I. Capillary Pressure. In *Developments in Petroleum Science*. 2015;64. Available: <https://doi.org/10.1016/B978-0-444-63533-4.00009-3>.
37. Schwartz B, Huffman K, Thornton D, Elsworth D. The effects of mineral distribution, pore geometry, and pore density on permeability evolution in gas; 2019.
38. Jennings H, Newman GH. Effect of temperature and pressure on the interfacial tension of water against methane- normal decane mixtures. *Soc Petrol Eng J*. 1971;11(2):171–175. Available: <https://doi.org/10.2118/3071-pa>.
39. Okasha TM, Aramco AAAS, Arabia S. Investigation of the Effect of Temperature and Pressure on Interfacial Tension and Wettability of Shu ' aiba reservoir , Saudi Arabia. 2006;3929.
40. Okasha TM, Aramco S. SPE 136934 Effect of Temperature and Pressure on Interfacial Tension and Contact Angle of Khuff Gas Reservoir, Saudi Arabia. Test; 2010.
41. Sarmadivaleh M, Al-Yaseri AZ, Iglauer S. Influence of temperature and pressure on quartz-water-CO<sub>2</sub> contact angle and CO<sub>2</sub>-water interfacial tension. *Journal of Colloid and Interface Science*. 2015;441:59–64.

- Available:<https://doi.org/10.1016/j.jcis.2014.11.010>.
42. Saraji S, Piri M, Goual L. The effects of SO<sub>2</sub> contamination, brine salinity, pressure, and temperature on dynamic contact angles and interfacial tension of supercritical CO<sub>2</sub>/brine/quartz systems. *International Journal of Greenhouse Gas Control*. 2014;28:147–155.
  43. Al-Bazali T. Insight on the inhibitive property of potassium ion on the stability of shale: a diffuse double-layer thickness ( $\kappa^{-1}$ ) perspective. *Journal of Petroleum Exploration and Production Technology*. 2021;11(6):2709-2723.
  44. Fauziah CA, Al-Yaseri AZ, Beloborodov R, Siddiqui MAQ, Lebedev M, Parsons D, Roshan H, Barifcani A, Iglauer S. Carbon Dioxide/Brine, Nitrogen/Brine, and Oil/Brine Wettability of Montmorillonite, Illite, and Kaolinite at Elevated Pressure and Temperature. *Energy and Fuels*. 2019;33(1):441–448.  
Available:<https://doi.org/10.1021/acs.energyfuels.8b02845>.
  45. Saraji S, Goual L, Piri M, Plancher H. Wettability of supercritical carbon dioxide/water/quartz systems: Simultaneous measurement of contact angle and interfacial tension at reservoir conditions. *Langmuir*. 2013;29(23):6856–6866.  
Available:<https://doi.org/10.1021/la3050863>.
  46. Al-Bazali TM, Zhang J, Chenevert ME, Sharma MM. A rapid, rigsite-deployable, electrochemical test for evaluating the membrane potential of shales. *SPE Drilling & Completion*. 2007;22(03):205–216.
  47. Talal AB. On CO<sub>2</sub> sequestration: changes in CO<sub>2</sub> entry pressure and adsorption capacity by heat. *Journal of Porous Media*. 2022;25(4):77-93.
  48. Akinwunmi B, Sun L, Hirvi JT, Kasa S, Pakkanen TA. Influence of temperature on the swelling pressure of bentonite clay. *Chemical Physics*. 2019;516:177–181.  
Available:<https://doi.org/10.1016/j.chemphys.2018.09.009>
  49. Teich-McGoldrick SL, Greathouse JA, Jové-Colón CF, Cygan RT. Swelling Properties of Montmorillonite and Beidellite Clay Minerals from Molecular Simulation: Comparison of Temperature, Interlayer Cation, and Charge Location Effects. *Journal of Physical Chemistry C*. 2015; 119(36):20880–20891.  
Available:<https://doi.org/10.1021/acs.jpcc.5b03253>.
  50. Vermeulen N. The water content of soils - Inaugural Lecture. 13th African Regional Conference on Soil Mechanics and Geotechnical Engineering; 2003.
  51. Al-Bazali TM. Membrane Efficiency Behavior in Shales (Doctoral dissertation); 2003.
  52. Jarrett MA, Gusler B, Xiang T, Clapper D. Improved Competence in Water Activity Measurement. AADE Technical Conference; 2004.